Supplementary Materials

Electrode switch—an efficient induced approach for self-activation of electrode toward water splitting

Jin Kong[a], Zhihong Wang[a]*, Chaoyue Liu[b], Shuo Wang[a], Yingshuang Guo[a], Honglei Chen[a] Jiepeng Wang[c, d], Zhe Lü[a]

[a.] *School of Physics, Harbin Institute of Technology, Yikuang Street 2#, Harbin, Heilongjiang 150001, People's Republic of China.*

[b.] *School of Science, Harbin University of Science and Technology, Heilongjiang 150080, People's Republic of China.*

[c.] *School of Materials Science and Engineering, Shanghai University, Shanghai 200444, People's Republic of China.*

[d.] *PERIC Hydrogen Technologies Co., Ltd, Handan 056000, People's Republic of China.*

** E-mail: wangzhihong@hit.edu.cn*

1. Experimental Section

1.1 Material Characterizations

The fresh Ni mesh (NM) was purchased from Heibei Chaochuang Company. Scanning electron microscopy (SEM, Hitachi S-4700) with an X-ray energy dispersive spectrometer (EDS) was used to observe the microstructure and elemental distribution of the sample. X-ray diffraction (XRD, X'Pert Pro (PANalytical)), Raman (Nano Base) spectrometers, electron paramagnetic resonance (EPR, German Bruker EMX PLUS) and X-ray photoelectron spectroscopy (XPS, Thermo Scientific K-Alpha) were used to characterize the phase, chemical state, and oxygen vacancies of the samples.

1.2 Electrochemical Measurement

Chronopotentiometry curves of two electrode systems were conducted to evaluate stability using Neware equipment (Shenzhen, China). The electrochemical performances of single electrodes were tested using a three-electrode setup and a CHI660E electrochemical workstation (Shanghai CH Instrument, China). NM, carbon rod, and Hg/HgO were used as the working electrodes, counter electrode, and reference electrode, respectively. These electrodes with a geometrical area of 1 cm^2 were used as the working electrode. 30% KOH solution was employed as the electrolyte for these tests. Linear sweep voltammetry (LSV) was measured with a potential window from 0 V to 1.0 V vs. Hg/HgO at a scan rate of 5 mV s^{-1} to evaluate the OER performances of the electrodes. Electrochemical impedance spectroscopy (EIS) was collected at a potential of 0.6 V vs. Hg/HgO with an amplitude of 5 mV. The frequency range used for the measurements was from 10^5 Hz to 0.01 Hz.

To evaluate the HER performances of the electrodes, linear sweep voltammetry (LSV) was measured with a potential window from -08 V to -1.8 V vs. Hg/HgO at a scan rate of 5 mV s^{-1}. Electrochemical impedance spectroscopy (EIS) was collected at a potential of -1 V vs. Hg/HgO with an amplitude of 5 mV. The frequency range used for the measurements was from 10^5 Hz to 0.01 Hz. The chronoamperometry (CP) method without iR compensation was also employed to evaluate stability using Neware equipment (Shenzhen, China).

To check the chemical reaction between the NM sample and the electrolyte, the NM electrode, immersed directly in the 30% KOH solution for 12 hours, was named immersion. Furthermore, these NM electrodes, after the 12 h OER and 12 h HER

polarization process in the 30% KOH solution at 300 mA cm^{-2}, were named OER 12h and HER 12h, respectively.

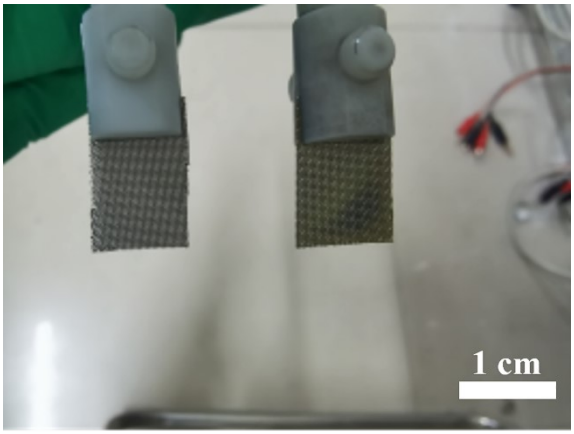

Fig. S1 Optical microscopy of fresh NM.

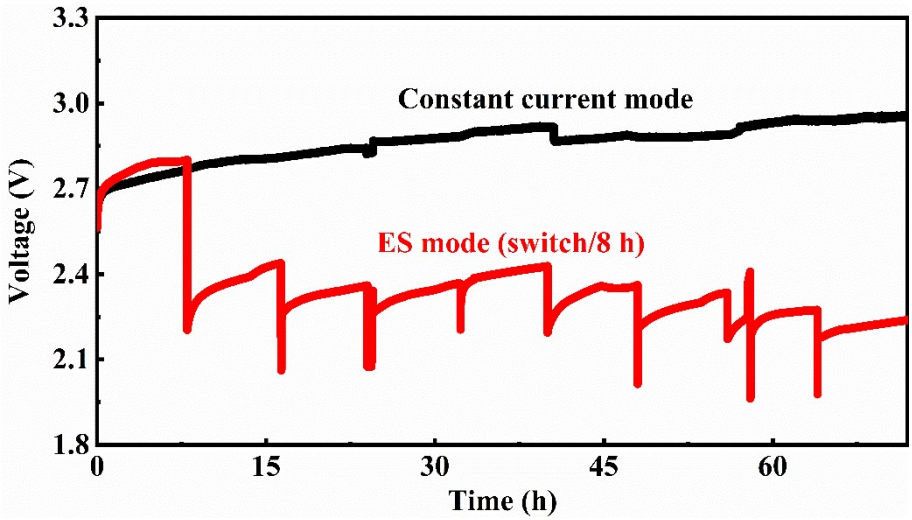

Fig. S2 Chronopotentiometry curves of NM electrodes under constant current and ES mode.

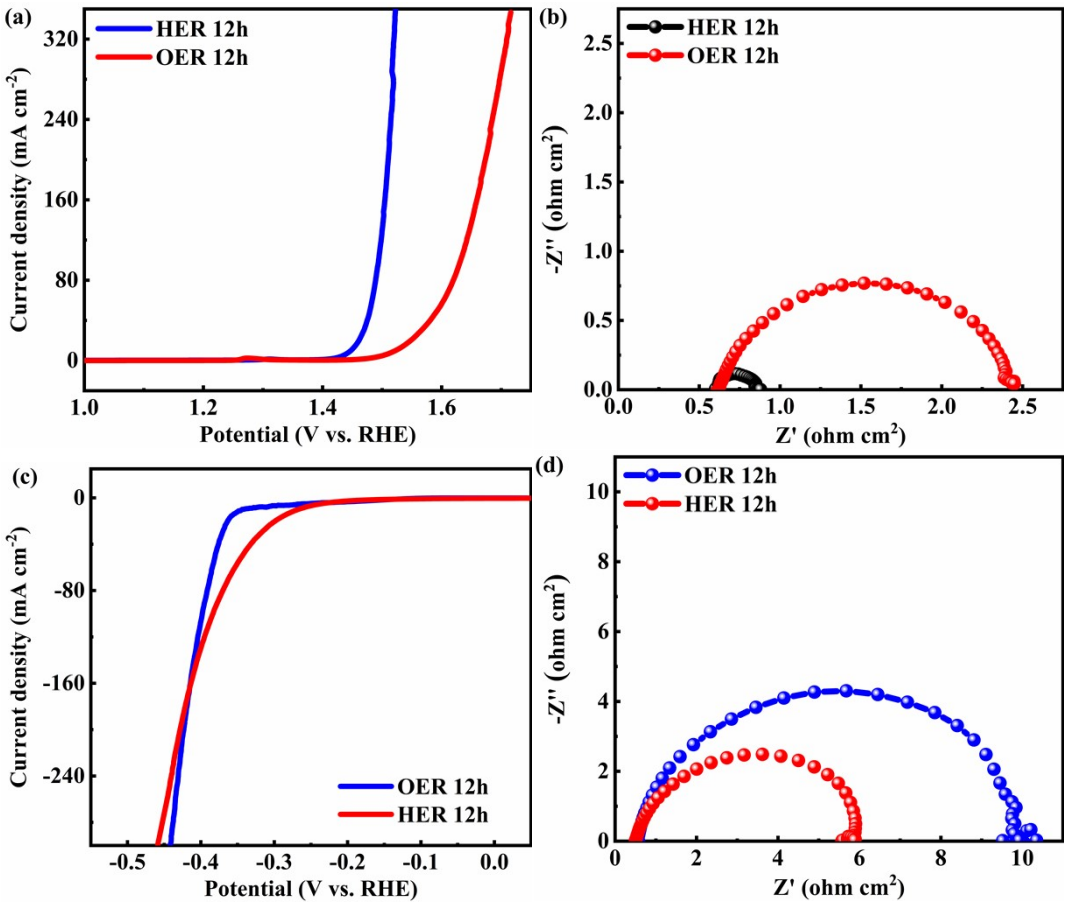

Fig. S3 (a) LSV curves and (b) EIS curves for OER of electrodes after OER polarization and HER polarization process. (c) LSV curves and (d) EIS curves for HER of electrodes after OER polarization and HER polarization process.

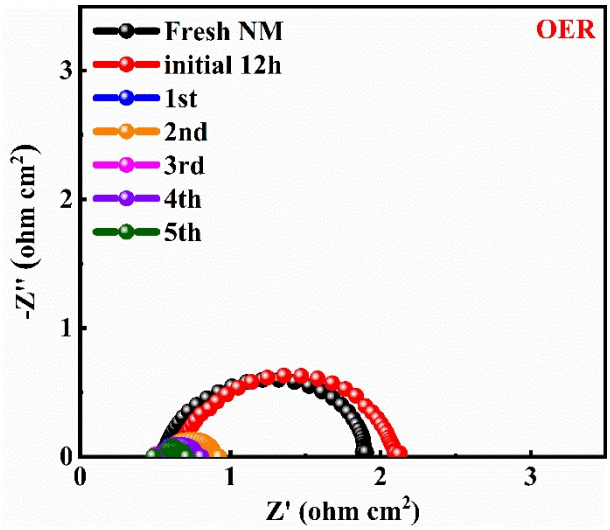

Fig. S4 EIS curves of the electrode in the process of OER after each switching process.

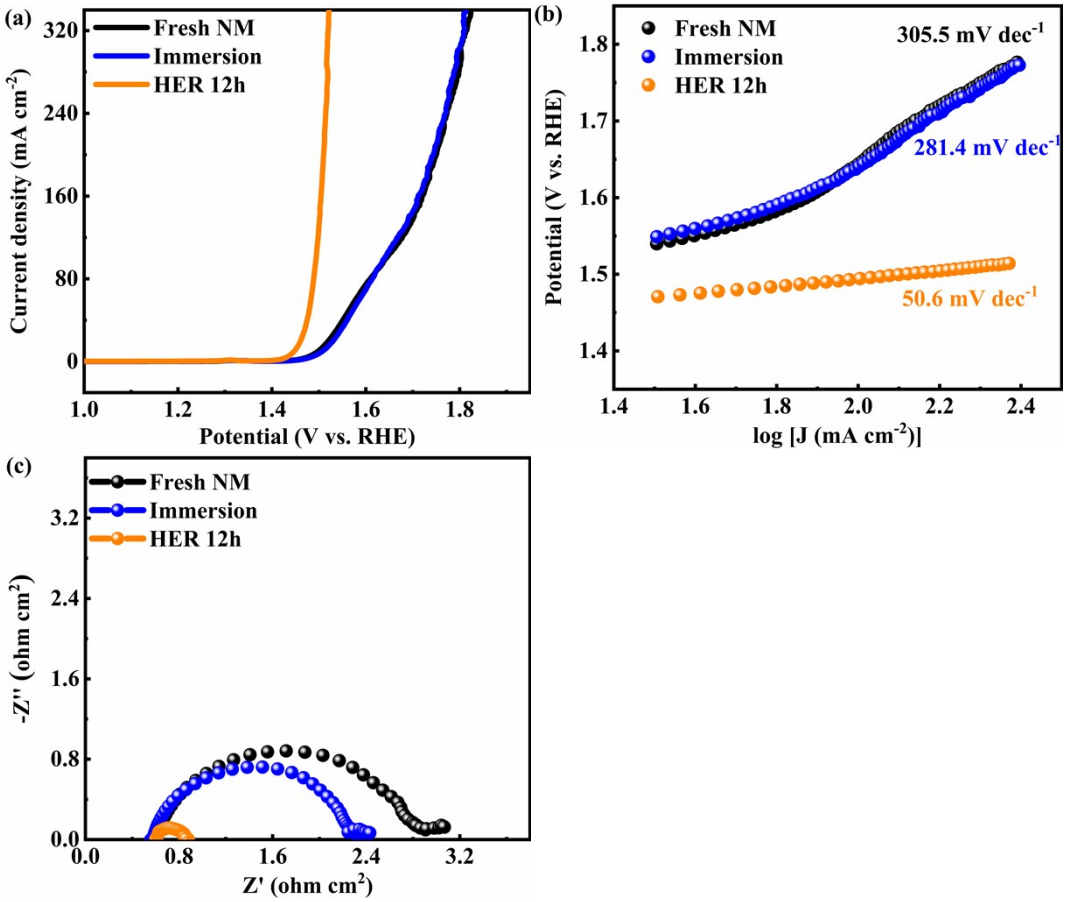

Fig. S5 (a) LSV curves, (b) Tafel plot curves, and (c) EIS curves for OER of fresh NM, NM immersing in KOH for 12h, and after the 12 h HER polarization process.

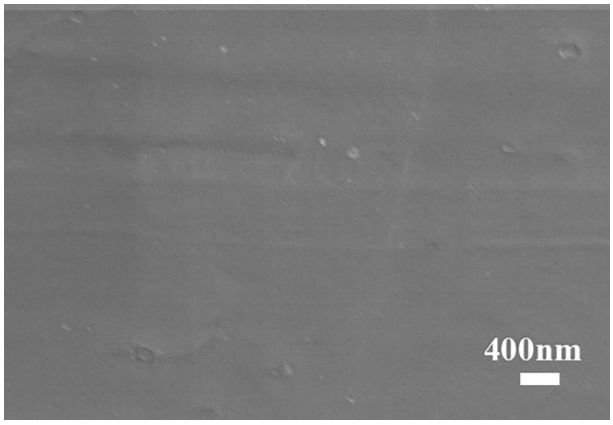

Fig. S6 SEM image of fresh NM.

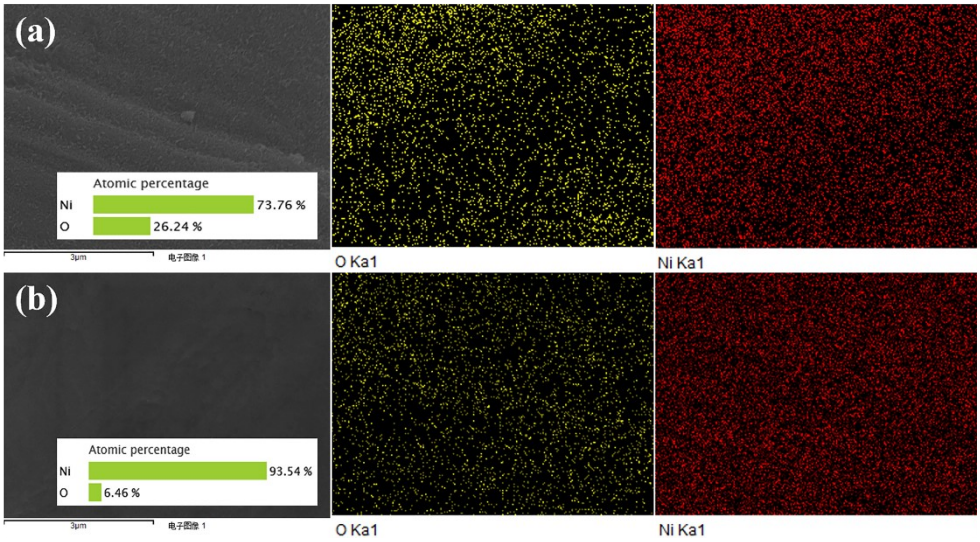

Fig. S7 EDS image of NM after (a) the OER polarization process and (b) an ES cycle.

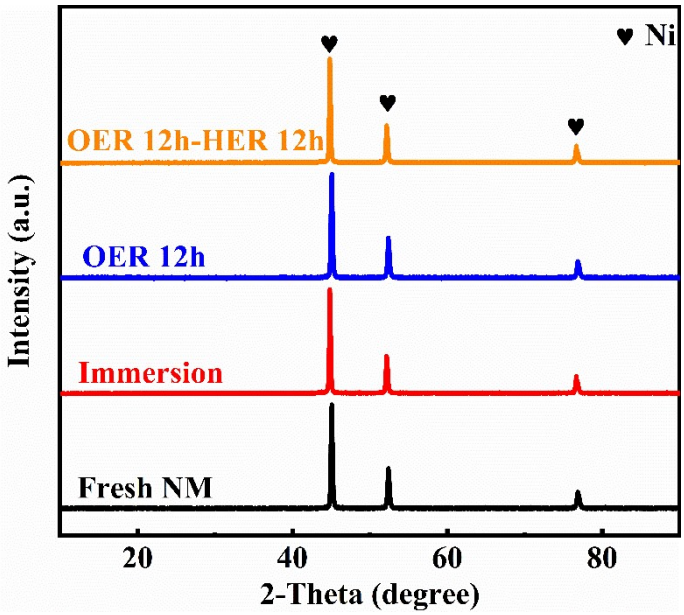

Fig. S8 XRD pattern of NM electrodes and NM electrodes for a typical cycle under the ES mode.

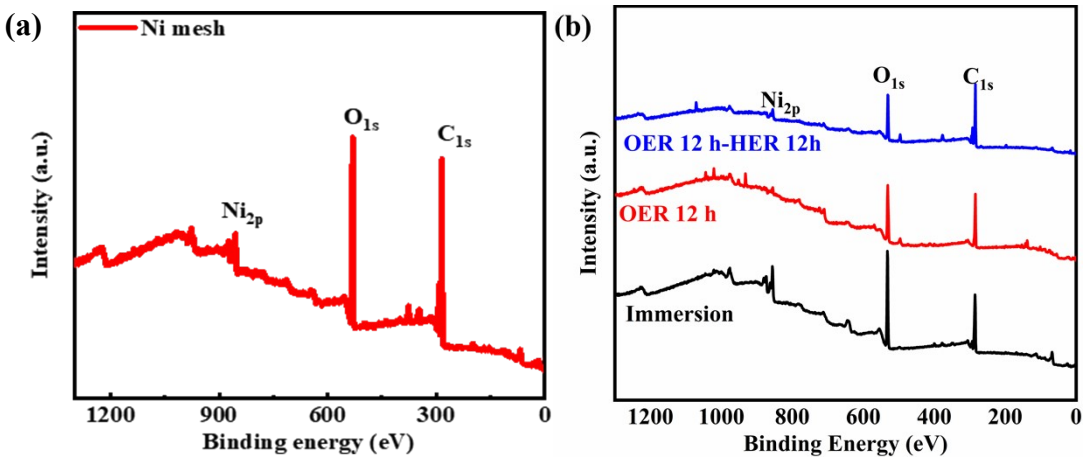

Fig. S9 XPS of (a) fresh NM and (b)the electrodes after each switching process.

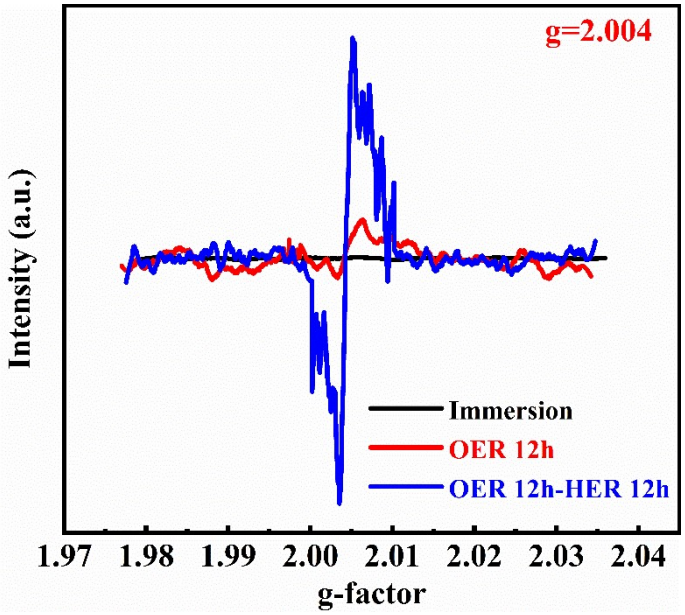

Fig.S10 EPR spectra of NM electrodes for a typical cycle under the ES mode.

Table.S1. Comparison of stability of overall water splitting performance

Anode	Cathode	Electrolyte	Current (mA/cm^2)	Time (h)	Degree of degrade	Ref.
NM	NM	4 M KOH	300	220	-8%	This work
d-(Fe,Ni)OOH/IF	NiMoN/NF	1 M KOH	500	100	4%	1
$Pd_{44}Pt_{30}Ir_{26}$ ASNSs/CC	$Pd_{44}Pt_{30}Ir_{26}$ ASNSs/CC	4 M KOH	125	40	6%	2
NiFeMo-OOH	Ru electrode	~6.9 M KOH	300	120	3%	3
NiFe_FA_NN	NiFeP_FA_NN	5 M KOH	1000	200	3%	4
Pt_1/CoHPO	Pt_1/CoHPO	0.1 M KOH	1000	100	0%	5
NiFeS@Ti_3C_2/NF	NiFeS@Ti_3C_2/NF	1 M KOH	401	35	0%	6
$Mo_{0.25}$NiFe/NF	$Mo_{0.25}$NiFe/NF	~6.9 M KOH	100	50	2%	7
$NiFe_2O_4$/SS fiber	Ni_3N/Ni/Ti mesh	1 M KOH	500	25	0%	8
Co, Mo-NiFe LDH/NF	Pt/C	~6.9 M KOH	400	130	1%	9
NiFe LDH/NiS/NF	Raney Ni	~6.9 M KOH	400	80	-	10
Mo-CoOOH/NF	20% Pt/C	1 M KOH	1000	100	12%	11
S-NiFe LDH	Pt@S-NiFe LDH	1 M KOH	500	150	3%	12

Supplementary References

1. L. Wu, M. Ning, X. Xing, Y. Wang, F. Zhang, G. Gao, S. Song, D. Wang, C. Yuan, L. Yu, J. Bao, S. Chen and Z. Ren, *Advanced Materials*, 2023, 35, 2306097.
2. Z. Lyu, X. Zhang, X. Liao, K. Liu, H. Huang, J. Cai, Q. Kuang, Z. Xie and S. Xie, *ACS Catalysis*, 2022, 12, 5305-5315.
3. B. Zhang, L. Wang, Z. Cao, S. M. Kozlov, F. P. García de Arquer, C. T. Dinh, J. Li, Z. Wang, X. Zheng, L. Zhang, Y. Wen, O. Voznyy, R. Comin, P. De Luna, T. Regier, W. Bi, E. E. Alp, C.-W. Pao, L. Zheng, Y. Hu, Y. Ji, Y. Li, Y. Zhang, L. Cavallo, H. Peng and E. H. Sargent, *Nature Catalysis*, 2020, 3, 985-992.
4. Z. Wei, M. Guo and Q. Zhang, *Applied Catalysis B: Environmental*, 2023, 322, 122101.
5. L. Zeng, Z. Zhao, F. Lv, Z. Xia, S.-Y. Lu, J. Li, K. Sun, K. Wang, Y. Sun, Q. Huang, Y. Chen, Q. Zhang, L. Gu, G. Lu and S. Guo, *Nature Communications*, 2022, 13, 3822.
6. D. Chanda, K. Kannan, J. Gautam, M. M. Meshesha, S. G. Jang, V. A. Dinh and B. L. Yang, *Applied Catalysis B: Environmental*, 2023, 321, 122039.
7. N. S. Gultom, T.-S. Chen, M. Z. Silitonga and D.-H. Kuo, *Applied Catalysis B: Environmental*, 2023, 322, 122103.
8. D. Zhang, H. Li, A. Riaz, A. Sharma, W. Liang, Y. Wang, H. Chen, K. Vora, D. Yan, Z. Su, A. Tricoli, C. Zhao, F. J. Beck, K. Reuter, K. Catchpole and S. Karuturi, *Energy & Environmental Science*, 2022, 15, 185-195.
9. Y. Zhao, Q. Wen, D. Huang, C. Jiao, Y. Liu, Y. Liu, J. Fang, M. Sun and L. Yu, *Advanced Energy Materials*, 2023, 13, 2203595.
10. Q. Wen, K. Yang, D. Huang, G. Cheng, X. Ai, Y. Liu, J. Fang, H. Li, L. Yu and T. Zhai, *Advanced Energy Materials*, 2021, 11, 2102353.
11. L. Tang, L. Yu, C. Ma, Y. Song, Y. Tu, Y. Zhang, X. Bo and D. Deng, *Journal of Materials Chemistry A*, 2022, 10, 6242-6250.
12. H. Lei, L. Ma, Q. Wan, S. Tan, B. Yang, Z. Wang, W. Mai and H. J. Fan, *Advanced Energy Materials*, 2022, 12, 2202522.